Implementation of a New MRAS Speed Sensorless Vector Control of Induction Machine

Idriss Benlaloui, Saïd Drid, *Senior Member, IEEE*, Larbi Chrifi-Alaoui, and Mohammed Ouriagli

***Abstract*—In this paper, a novel rotor speed estimation method using model reference adaptive system (MRAS) is proposed to improve the performance of a sensorless vector control in the very low and zero speed regions. In the classical MRAS method, the rotor flux of the adaptive model is compared with that of the reference model. The rotor speed is estimated from the fluxes difference of the two models using adequate adaptive mechanism. However, the performance of this technique at low speed remains uncertain and the MRAS loses its efficiency, but in the new MRAS method, two differences are used at the same time. The first is between rotor fluxes and the second between electromagnetic torques. The adaptive mechanism used in this new structure contains two parallel loops having Proportional-integral controller and low-pass filter. The first and the second loops are used to adjust the rotor flux and electromagnetic torque. To ensure good performance, a robust vector control using sliding mode control is proposed. The controllers are designed using the Lyapunov approach. Simulation and experimental results show the effectiveness of the proposed speed estimation method at low and zero speed regions, and good robustness with respect to parameter variations, measurement errors, and noise is obtained.**

***Index Terms*—Induction motor, Lyapunov function, model reference adaptive system (MRAS), sensorless control, speed estimation, vector control.**

NOMENCLATURE

s, r	Rotor and stator indices.
d, q	Direct and quadrate indices for orthogonal components.
$\bar{x}$	Variable complex such as: $\bar{x} = \Re e\,[\bar{x}] + j.\Im m\,[\bar{x}]$ with $j^2 = -1$.
$\bar{x}$	It can be a voltage as $\bar{u}$, a current as $\bar{i}$ or a flux as $\bar{\varphi}$.
$\bar{x}^*$	Complex conjugate.
R_s, R_r	Stator and rotor resistances.
L_s, L_r	Stator and rotor inductances.
T_s,T_r	Stator and rotor time-constants ($T_{sr} = L_{s,r}/R_{s,r}$).
σ	Leakage flux total coefficient ($\sigma = 1 - M^2/L_r L_s$).
M	Mutual inductance.
P	Number of pole pairs.
ω	Mechanical rotor frequency (rd/s).
Ω	Rotor speed (rd/s).
ω_s	Stator current frequency (rd/s).
ω_r	Induced rotor *current* frequency (rd/s).
ω_c	Injected rotor current frequency (rd/s).
J_in	Inertia.
f	Coefficient of viscous.
Γ	Unknown torque.
Γ_e,Γ_max	Electromagnetic torque and maximal torque.
$\sim$	Symbol indicating measured value.
$\wedge$	Symbol indicating the estimated value.
$*$	Symbol indicating the command value.
IM	Induction motor.
MRAS	Model reference adaptive system.

Manuscript received May 6, 2014; revised September 29, 2014 and July 16, 2014; accepted October 21, 2014. Date of publication November 20, 2014; date of current version May 15, 2015. Paper no. TEC-00310-2014.

I. Benlaloui and S. Drid are with the Laboratory of Induction and Propulsion Systems, Electrical Engineering Department, University of Batna, Batna 05000, Algeria (e-mail: idrissb88@yahoo.fr; s_drid@yahoo.fr).

L. Chrifi-Alaoui is with of the University of Picardie Jules Verne, 02880 Cuffies, France (e-mail: larbi.alaoui@u-picardie.fr).

M. Ouriagli is with the Laboratoire d'Informatique Mathématiques Automatique et Optoélectronique, Faculté Polydisciplinaire de Taza Maroc, B.P. 1223 Taza, Morocco (e-mail: omenstz@yahoo.fr).

Digital Object Identifier 10.1109/TEC.2014.2366473

I. INTRODUCTION

SPEED INFORMATION is mandatory for the operation of vector-controlled induction motor (IM) drive. The rotor speed can be measured through a sensor or may be estimated using voltage, current signals, and machine parameters. The use of speed sensor is associated with problems, such as, reduction of mechanical robustness of the drive, need of shaft extension, reliability reduction, and cost increase. Therefore, a speed sensorless drive has a clear edge over the traditional vector-controlled drive.

Several speed estimators for sensorless vector control of induction motor have been proposed as summarized recently in [1]. They can be divided into two groups, the model-based estimators and signal injection-based estimators. Among the first group, the MRAS, the adaptive Luenberger observers and the extended Kalman-filter. The main drawback of these model-based estimators is their insufficient performance at low speeds and parameters machine sensitivity. In order to overcome these problems, signal injection-based methods [2], [3] were developed. Although these methods perform well at low and zero speed regions, they suffers from, computational complexity, the need of external hardware for signal injection and the adverse effect of injecting signal on the machine performance. Therefore, due to their simplicity, model-based methods and especially MRAS-based methods are, until now, the most widely used.

Numerous MRAS-based on rotor flux, back electromotive force, reactive power, and outer product of stator voltage–current ($\bar{v}_s^* \otimes \bar{i}_s^*$)[4]–[10] have been proposed. However, rotor flux MRAS first introduced by Schauder [11], [5], remain the most popular MRAS strategy, and a lot of effort has been focused on improving its performance [1]. Indeed, the drawbacks of this technique are parameter sensitivity, especially to stator resistance, and pure integration problems [6], [12]–[14], which limit its performance at low and zero speed regions of operation.

Many solutions have been proposed to improve the performance at and around zero speed, among them, online adaptation of the stator resistance [15], simultaneous MRAS estimation of speed, and stator resistance [16]. Also, to overcome pure integration problems, low-pass filters (LPF) [17], [18] with low cutoff frequency and a programmable cascaded LPF [19] were used.

This paper proposes a field-oriented control (FOC) induction motor drive based on a new MRAS method. First, the modeling of the induction machine is described. Then, a sliding-mode controller is designed to ensure good and robust performance with respect to parameters variations, and a new MRAS rotor speed observer is proposed. Finally, experimental results are discussed.

II. The IM Model

The Induction machine dynamic model expressed in the synchronous reference frame is given by voltage equations

$$\begin{cases} \bar{u}_s = R_s\bar{I}_s + \sigma L_s\dfrac{d\bar{I}_s}{dt} + \dfrac{M}{L_r}\dfrac{d\bar{\phi}_r}{dt} + j\sigma L_s\omega_s\bar{I}_s \\ \qquad + j\dfrac{M}{L_r}\omega_s\bar{\phi}_r \\ 0 = \dfrac{1}{T_r}\bar{\phi}_r - \dfrac{M}{T_r}\bar{I}_s + \dfrac{d\bar{\phi}_r}{dt} + j\omega_r\bar{\phi}_r \end{cases}. \tag{1}$$

The motion equation is

$$\Gamma_e - \Gamma_l = J_{\text{in}}\frac{d\Omega}{dt} + f\Omega. \tag{2}$$

where the electromagnetic torque is

$$\Gamma_e = \frac{\text{PM}}{L_r}(I_{sq}\phi_{rd} - I_{sd}\phi_{rq}). \tag{3}$$

If we assume that the torque load and the viscous coefficient are unknown, we can write

$$\Gamma_e - \Gamma = J_{\text{in}}\frac{d\Omega}{dt}, \tag{4}$$

where $\Gamma = \Gamma_l + f\Omega$.

III. Vector Control Strategy

A. Rotor Flux Orientation

The objective of flux rotor orientation or vector control is to decouple the stator current into flux and torque producing components, regulated separately, to obtain a good performance IM drive [20], [21]. Then

$$\begin{cases} \phi_{rq} = 0 \\ \phi_{rd} = \varphi_r \end{cases}. \tag{5}$$

Using (5), the developed torque given by (3) can be rewritten as follows:

$$\Gamma_e = k_c\phi_r I_{sq} \tag{6}$$

where $k_c = \frac{\text{PM}}{L_r}$, and I_{sq} appears as the input command of the active power or simply of the developed torque, while I_{sd} appears as the input command of the reactive power.

B. Robust Control Law Design

Separating the real and the imaginary part of (1), we can write

$$\begin{cases} \frac{dI_{sd}}{dt} = h_1 + \gamma_1 u_{sd} \\ \frac{dI_{sq}}{dt} = h_2 + \gamma_1 u_{sq} \\ \frac{d\Omega}{dt} = h_3 + \gamma_2 u_T \end{cases} \tag{7}$$

*w*here h_1, h_2, and h_3 are done as follows:

$$\begin{cases} h_1 = \gamma_1\left(-R_sI_{sd} - \dfrac{M}{L_r}\dfrac{d\phi_{rd}}{dt} + \sigma L_s\omega_s I_{sq} + \dfrac{M}{L_r}\omega_s\phi_{rq}\right) \\ h_2 = \gamma_1\left(-R_sI_{sq} - \dfrac{M}{L_r}\dfrac{d\bar{\phi}_r}{dt} + \sigma L_s\omega_s I_{sd} - \dfrac{M}{L_r}\omega_s\phi_{rd}\right) \\ h_3 = -\dfrac{1}{J_{\text{in}}}\left(\Gamma + P\dfrac{M}{L}\phi_{rq}I_{sd}\right) \end{cases} \tag{8}$$

with $\gamma_1 = \frac{1}{\sigma L_s}$, $\gamma_2 = \frac{k_c\phi_{rd}}{J_{\text{in}}}$ and the virtual control $u_T = I^*_{sq}$.

The functions h_1, h_2, and h_3 involved in the model of induction motor (IM) are strongly affected by the temperature, the saturation, and the skin effect in addition of the different nonlinearities related to harmonic pollution due to supplying converters and to noise measurements. In this section, our objective is to design a robust control law, which can take into account all these effects and guarantee a good performance. In general, we can write

$$\begin{cases} h_1 = \hat{h}_1 + \Delta h_1 \\ h_2 = \hat{h}_2 + \Delta h_2 \\ h_3 = \hat{h}_3 + \Delta h_3 \end{cases} \tag{9}$$

where $\hat{h}_{1,2,3}$: nominal functions, $h_{1,2,3}$: actual functions, $\Delta h_{1,2,3}$: variations around nominal functions.

In this case, the load torque Γ is unknown but limited i.e., $|\Gamma| \leq \Gamma_{\max}$ and magnetizing flux ϕ_{rd} is nonzero (remanence flux).

We assume that all $\Delta h_{1,2,3}$ are bounded as follows:

$$\begin{cases} |\Delta h_1| < \zeta_1 \\ |\Delta h_2| < \zeta_2 \\ |\Delta h_3| < \zeta_3 \end{cases}. \tag{10}$$

Replacing (9) in (7), we obtain

$$\begin{cases} \dfrac{dI_{sd}}{dt} = \hat{h}_1 + \Delta h_1 + \gamma_1 u_{sd} \\ \dfrac{dI_{sq}}{dt} = \hat{h}_2 + \Delta h_2 + \gamma_1 u_{sq} \\ \dfrac{d\Omega}{dt} = \hat{h}_3 + \Delta h_3 + \gamma_2 u_T \end{cases}. \tag{11}$$

We can formulate the Lyapunov function as follows [22]–[24]:

$$V = \frac{1}{2}e_d^2 + \frac{1}{2}e_q^2 + \frac{1}{2}e_\omega^2 > 0 \tag{12}$$

where $e_d = (I_{sd} - I^*_{sd})$, $e_q = (I_{sq} - I^*_{sq})$, and $e_\omega = (\Omega - \Omega^*)$.

The derivative of the Lyapunov function (12) becomes

$$\dot{V} = \dot{e}_d e_d + \dot{e}_q e_q + \dot{e}_\omega e_\omega. \tag{13}$$

Substituting (7) in (13), it results

$$\begin{aligned}\dot{V} = \; & (\hat{h}_1 + \Delta h_1 + \gamma_1 u_{sd} - \dot{I}^*_{sd}) e_d \\ & + (\hat{h}_2 + \Delta h_2 + \gamma_1 u_{sq} - \dot{I}^*_{sq}) e_q \\ & + (\hat{h}_3 + \Delta h_3 + \gamma_2 u^*_T - \dot{\Omega}^*) e_\omega. \end{aligned} \tag{14}$$

Let us define the following law control as:

$$\begin{aligned} u_{sd} &= -\alpha_1 \hat{h}_1 + \alpha_1 \dot{I}^*_{sd} - \alpha_1 K_1 e_d - \alpha_1 K_{11} \mathrm{sgn}(e_d) \\ u_{sq} &= -\alpha_1 \hat{h}_2 + \alpha_1 \dot{I}^*_{sq} - \alpha_1 K_2 e_q - \alpha_1 K_{22} \mathrm{sgn}(e_q) \\ u_T &= -\alpha_2 \dot{\Omega} - \alpha_2 K_3 e_\omega - \alpha_2 K_{33} \mathrm{sgn}(e_\omega) \end{aligned} \tag{15}$$

where $\alpha_1 = \frac{1}{\gamma_1}$, $\alpha_2 = \frac{1}{\gamma_2}$.

Hence, (15) replaced in (14) gives

$$\begin{aligned}\dot{V} = \; & -K_1 e_d^2 - K_2 e_q^2 - K_3 e_\omega^2 \\ & + (\Delta h_1 - K_{11} \mathrm{sgn}(e_d)) e_d \\ & + (\Delta h_2 - K_{22} \mathrm{sgn}(e_d)) e_q \\ & + (\hat{h}_3 + \Delta h_3 - K_{33} \mathrm{sgn}(e_\omega)) e_\omega. \end{aligned} \tag{16}$$

Hence, the $\Delta h_{1,2,3}$ variations can be absorbed if we take

$$\begin{aligned} K_{11} &> |\Delta h_1| \\ K_{22} &> |\Delta h_2| \\ K_{33} &> \left| \hat{h}_3 + \Delta h_3 \right|. \end{aligned} \tag{17}$$

The latter inequalities are satisfied since $K_{1,2,3} > 0$ and

$$\begin{aligned} |\Delta h_1| &< \zeta_1 < K_{11} \\ |\Delta h_2| &< \zeta_2 < K_{22} \\ \left| \hat{h}_3 + \Delta h_3 \right| &< |\Gamma| + |\zeta_3| < K_{33}. \end{aligned} \tag{18}$$

Finally, we can write

$$\dot{V} < 0. \tag{19}$$

Hence, using the Lyapunov theorem [22]–[24], we conclude that

$$\begin{cases} \lim\limits_{t \to +\infty} e_d = 0 \\ \lim\limits_{t \to +\infty} e_q = 0 \\ \lim\limits_{t \to +\infty} e_\omega = 0 \end{cases}. \tag{20}$$

IV. MRAS Speed Observer

The MRAS approach uses two models. The model that does not involve the quantity to be estimated (the rotor speed) is considered as the reference model. The model that has the quantity to be estimated involved is considered as the adaptive model (or adjustable model). The outputs obtained with the two models are compared, and the difference is used to derive a suitable adaptive mechanism whose output is the quantity to be estimated (rotor speed in our case). The adaptive mechanism should be designed to ensure the stability of the controlled system. Fig. 1 illustrates the basic structure of MRAS [20], [25], [21].

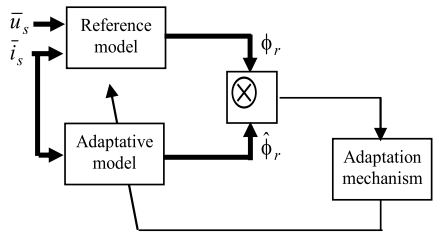

Fig. 1. Classical rotor flux MRAS speed observer.

The induction motor model can be represented in the stator reference frame as follows:

$$\begin{cases} \bar{u}_s = R_s \bar{i}_s + \sigma L_s \frac{d\bar{i}_s}{dt} + \frac{M}{L_r} \frac{d\bar{\phi}_r}{dt} \\ 0 = \frac{1}{T_r} \bar{\phi}_r - \frac{M}{T_r} \bar{i}_s + \frac{d\bar{\phi}_r}{dt} - jP\Omega \bar{\phi}_r \end{cases}. \tag{21}$$

A. Classical MRAS Speed Observer

The MRAS speed observer analyzed two independent equations for the derivative time of rotor flux vector, obtained from (1) in the stationary reference frame (α, β). They are usually referred to as the "voltage model" and "current model," and they are given, respectively, by

$$\bar{\phi}_r = \frac{\sigma L_s L_r}{M} \bar{i}_s + \frac{L_r}{M} \int (\bar{u}_s - R_s \bar{i}_s) dt \tag{22}$$

and

$$\bar{\phi}_r = \int \left(\frac{M}{T_r} \bar{i}_s - \left(\frac{1}{T_r} - jP.\Omega \right) \bar{\phi}_r \right) dt. \tag{23}$$

For the same input $\bar{i}_s$, (23) can be written in an estimated form

$$\hat{\bar{\phi}}_r = \int \left(\frac{M}{T_r} \bar{i}_s - \left(\frac{1}{T_r} - jP.\hat{\Omega} \right) \hat{\bar{\phi}}_r \right) dt. \tag{24}$$

The dynamic equation of the estimation error $\bar{e}_\phi = (\bar{\phi}_r - \hat{\bar{\phi}}_r)$ is obtained by subtracting (23) and (24)

$$\dot{\bar{e}}_\phi = -\left(\frac{1}{T_r} - jP.\Omega \right) \bar{e}_\phi + jP(\Omega - \hat{\Omega}) \hat{\bar{\phi}}_r. \tag{25}$$

It is important to ensure that the system (25) is stable, which naturally requires the error (e_ϕ) to be close to zero. As noted in [11], the stability of this algorithm is studied, using the hyperstability Popov criterion. Indeed, the derivation of the error is composed of two terms. The first is linear and the second is nonlinear.

In matrix form, this differential equation is written as

$$\dot{\bar{e}}_\phi = A \bar{e}_\phi - W \tag{26}$$

where

$$A = -\frac{1}{T_r} I + J.P\Omega; \qquad W = J.P(\Omega - \hat{\Omega}) \hat{\bar{\phi}}_r = J.P\Delta\Omega \hat{\bar{\phi}}_r$$

$$\bar{e}_\phi = \begin{bmatrix} \phi_{r\alpha} - \hat{\phi}_{r\alpha} \\ \phi_{r\beta} - \hat{\phi}_{r\beta} \end{bmatrix}; \text{ and } I = \begin{bmatrix} 1 & 0 \\ 0 & 1 \end{bmatrix}; \qquad J = \begin{bmatrix} 0 & -1 \\ 1 & 0 \end{bmatrix}.$$

A is a Hurwitz matrix (stable). According to the Lyapunov function of the linear part $\dot{\bar{e}}_\phi = A\bar{e}_\phi$, we get

$$V = \bar{e}_\phi^T \bar{e}_\phi > 0. \tag{27}$$

The derivative of the Lyapunov function becomes

$$\dot{V} = \dot{\bar{e}}_\phi^T \bar{e}_\phi + \bar{e}_\phi^T \dot{\bar{e}}_\phi = \bar{e}_\phi^T (A^T + A)\bar{e}_\phi = -\frac{2}{T_r}\bar{e}_\phi^T \bar{e}_\phi. \tag{28}$$

The function given in (28) is globally negative definite.Thus, $\dot{V} < 0 \quad \forall \Omega$.

We can obtain the adaptive mechanism by Lyapunov, but it is simpler to be extracted from Popov's criterion

$$\int_0^t e_\phi^T W d\tau = \int_0^t (P\Delta\Omega[\, e_{\phi\alpha} \quad e_{\phi\beta}\,] J\hat{\bar{\phi}}_r) d\tau \geq -\delta_o^2. \tag{29}$$

Assuming the speed changes very slowly with the same theorem of parameter analysis mentioned above, we can write

$$\begin{aligned} \hat{\Omega} &= \delta_0 P \int [\, e_{\phi\alpha} \quad e_{\phi\beta}\,] J\hat{\bar{\phi}}_r dt \\ &= \delta_0 P \int (e_{\phi\beta}\hat{\phi}_{r\alpha} - e_{\phi\alpha}\hat{\phi}_{r\beta}) dt. \end{aligned} \tag{30}$$

The adaptation law has open-loop integration (offset problem). To improve the estimation response, an LPF was proposed by many authors [26] and [27]. Then, (30) becomes

$$\hat{\Omega} = k_p(\bar{\phi}_r \otimes \hat{\bar{\phi}}_r) + k_i \int (\bar{\phi}_r \otimes \hat{\bar{\phi}}_r) dt \tag{31}$$

where k_p and k_i are positive gains.

However, the main problem of the classical MRAS observer is its poor estimation at low speeds [1]. That is why we present a new MRAS speed observer in the following paragraph.

B. New MRAS Speed Observer

In the new MRAS method, two differences are used on the same time. The first is between rotor fluxes, and the second is between electromagnetic torques.

Indeed, the electromagnetic torque can be expressed as

$$\Gamma_e = P\frac{M}{L_r}(\bar{i}_s \otimes \bar{\phi}_r) \tag{32}$$

where $\bar{\phi}_r$ is given by (23).

The estimated electromagnetic torque can be expressed as

$$\hat{\Gamma}_e = P\frac{M}{L_r}(\bar{i}_s \otimes \hat{\bar{\phi}}_r) \tag{33}$$

where $\hat{\bar{\phi}}_r$ is given by (24).

It is well established that the motion equation (2) governs the mechanical dynamics part of the machine, then a variation of the load results in a variation of the speed until the electromagnetic torque becomes equal to the load torque.

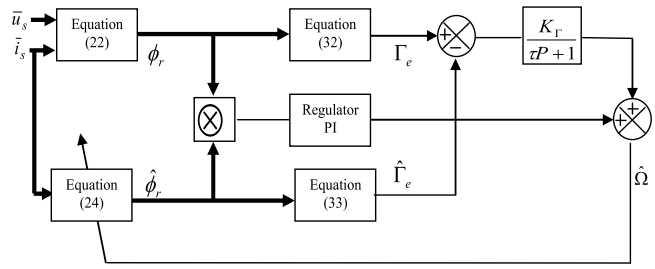

Fig. 2. Block diagram of the new MRAS observer.

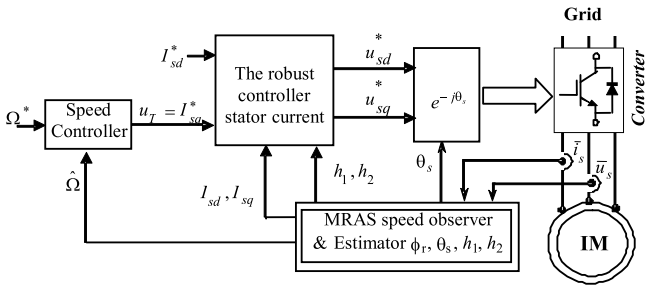

Fig. 3. Block diagram of sensorless field-oriented control system.

Based on the same principle, a variation in the estimated torque results in a variation of the estimated speed until the estimated torque becomes equal to the electromagnetic torque.

Then, by using the mechanical equation (2) and by replacing the electromagnetic torque and the speed by their estimated values, we can write

$$\hat{\Gamma}_e - \Gamma_l = J_{\text{in}}\frac{d\hat{\Omega}}{dt} + f\hat{\Omega}. \tag{34}$$

By subtracting (34) from (2), we obtain the following equation:

$$e_\Gamma = \Gamma_e - \hat{\Gamma}_e = J_{\text{in}}\frac{d(\Omega - \hat{\Omega})}{dt} + f(\Omega - \hat{\Omega}). \tag{35}$$

Then, for good speed estimation, we must take into account the two following conditions:

$$\begin{cases} \dot{\bar{e}}_\phi = -\left(\frac{1}{T_r} - jP\Omega\right)\bar{e}_\phi + jP(\Omega - \hat{\Omega})\hat{\bar{\phi}}_r \\ e_\Gamma = \Gamma_e - \hat{\Gamma}_e = J_{\text{in}}\frac{d(\Omega - \hat{\Omega})}{dt} + f(\Omega - \hat{\Omega}) \end{cases}. \tag{36}$$

With the same way that we determinate the adaptation law previously and with taking into account the error of torque the adaptation becomes

$$\hat{\Omega} = \left(K_p + \frac{K_i}{p}\right)(\bar{\phi}_r \otimes \hat{\bar{\phi}}_r) + K_\Gamma \frac{e_\Gamma}{\tau p + 1} \tag{37}$$

where τ is chosen to be close to the mechanical time constant.

In this scheme, the electromagnetic torque error $e_\Gamma = (\Gamma_e - \hat{\Gamma}_e)$, is filtered by the LPF and added to the classical adaptation law loop. The new MRAS observer block diagram is given in Fig. 2.

Fig. 3 illustrates a general block diagram of the suggested IM control scheme.

TABLE I
GAINS OF CONTROLLERS

Controller	Gains
I_{sd}-Controller	$K1 = 300; K11 = 25$
I_{sq}-Controller	$K2 = 750; K22 = 50$
Speed-Controller	$K3 = 500; K33 = 10$
PI-Observer	$k_p = 1000; k_i = 10000$
New-MRAS Filter	$K_\Gamma = 333, \tau = 1.63$

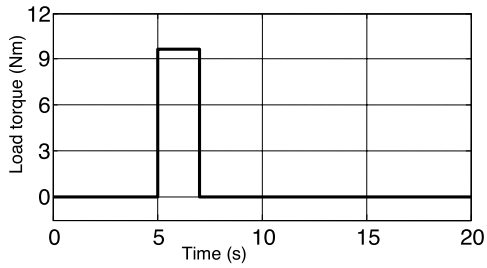

Fig. 4. Load torque variation.

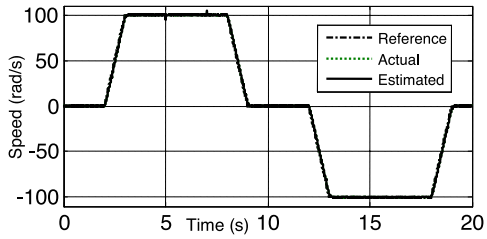

Fig. 5. Speed of induction motor.

V. SIMULATION AND EXPERIMENTAL IMPLEMENTATION

In this section, the performance of the proposed observer structure is presented via simulation and experimental results. First, the performances of the proposed observer are analyzed and compared with the classical MRAS observer by simulation. Second, to validate the simulation results, extensive experimentations are conducted by using dSPACE DS1104. The rating and parameters of the induction motor are given in the appendix, the values of all controllers gains are given in Table I.

A. Simulation Results

A sensorless FOC induction motor drive, shown in Fig. 3, is used where the actual speed feedback signal is replaced by the estimated one. Fig. 5 shows reference, actual, and estimated speed. We can see in Figs. 6 and 7 that the speed estimation error (error between actual and estimated speed) and tracking speed error (error between reference and estimated speed) are small even at zero speed regions and converge quickly to zero. To test the robustness toward load torque variation at a constant speed reference, a step load variation of 10 Nm (see Fig. 4) is applied between $t = 5$ s and $t = 7$ s. As we can see, after small variations, the estimation and tracking speed errors converge to zero. All these results confirm the efficiency of our speed observer and control. Also, in order to confirm the field orientation, *d*- and *q*-axis flux are separately shown in Fig. 8. We can see that the *q*-axis flux is maintained at zero value.

The sensitivity to stator resistance mismatch and load torque variation of the proposed new MRAS method and the classical MRAS is shown in Figs. 9–11 for $+20\%$ *Rs* variations and 10-Nm load variation at low speeds. As can be observed, while the tracking performance of the two methods seems to be satisfactory (see Fig. 10), the accuracy of the new MRAS observer is

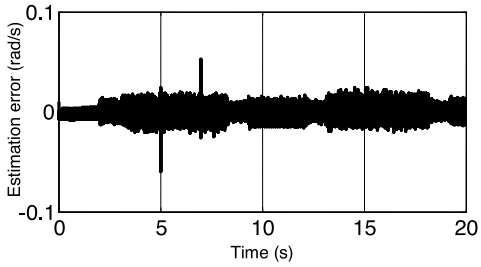

Fig. 6. Speed estimation error.

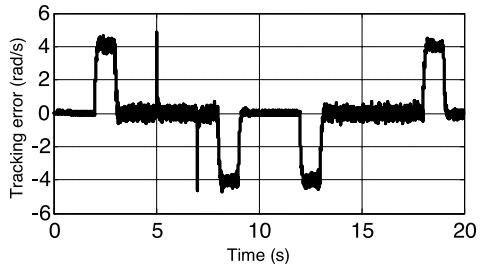

Fig. 7. Speed tracking error.

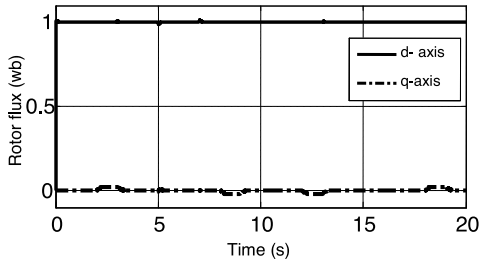

Fig. 8. Rotor flux.

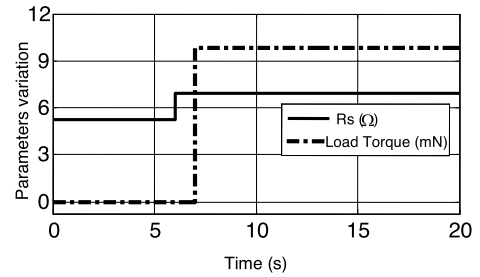

Fig. 9. Load torque and *Rs* variations.

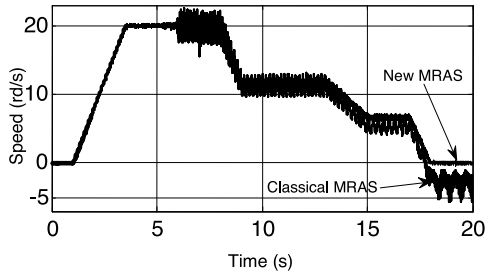

Fig. 10. Classical MRAS observer: Reference, actual, and estimated speed for load torque and *Rs* variations.

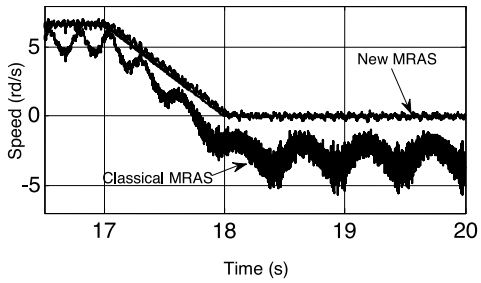

Fig. 11. Classical MRAS observer: Zoom of Reference, actual, and estimated speed for load torque and *Rs* variations.

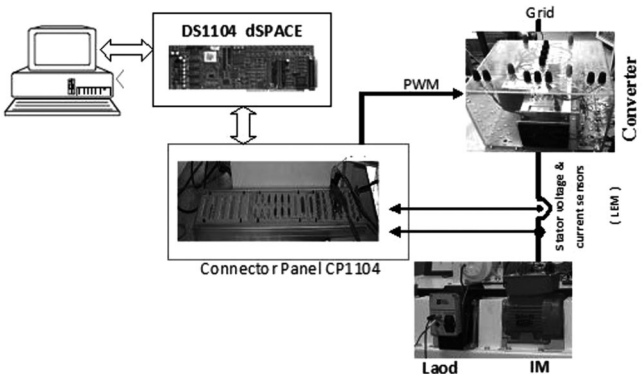

Fig. 12. Structure of the laboratory setup.

much better than this of the classical one especially at low speed (see Fig. 11).

B. Description of the Laboratory Setup

The basic structure of the laboratory setup is depicted in Fig. 12. The DC machine is used as a load. The IM stator is fed by a SEMIKRON converter (4 kW, IGBT modules) controlled directly by the DS1104 board. The dSPACE DS1104 PPC is plugged in the host PC. The encoder is used to measure the mechanical speed. The sensors are used for the currents and voltages measures are, respectively, LA-55NP and LV-25P. The Interface is used to provide galvanic isolation to all signals connected to the DS1104 PPC controller.

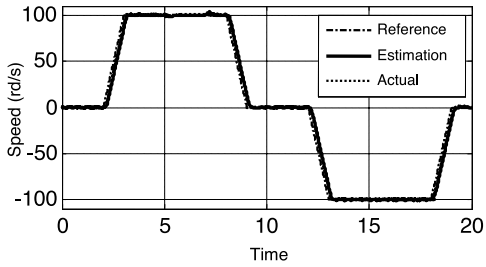

Fig. 13. Speed of induction motor.

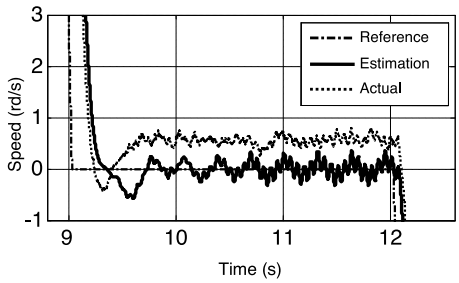

Fig. 14. Speed zoom.

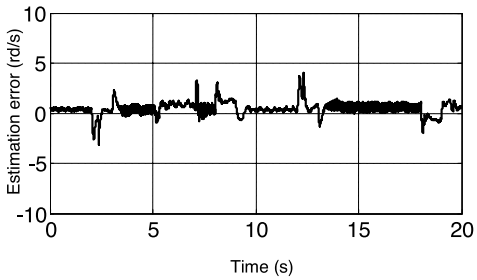

Fig. 15. Speed estimation error.

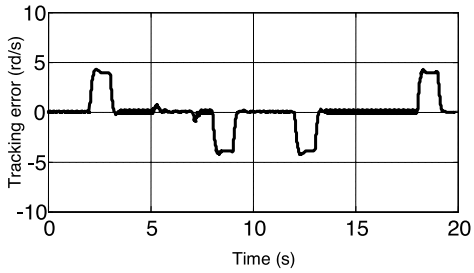

Fig. 16. Speed tracking error.

C. Experimental Results

Fig. 13 shows the reference, measured (actual), and estimated speed and also the speed reference of the proposed sensorless control. We can see that the measured and estimated speed are close to each other and converge to the speed reference. In Figs. 14–16, we show that the measured and tracking speed errors are small and converge quickly to zero even at zero speed. These experimental results prove the efficiency of our proposed observer and control and confirm the simulation results. In order

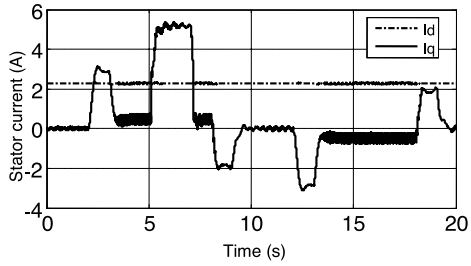

Fig. 17. I_{sd} and I_{sq} stator currents.

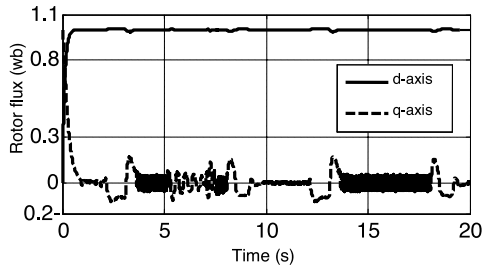

Fig. 18. Rotor flux.

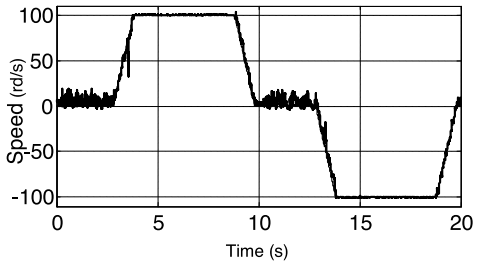

Fig. 19. Classical MRAS: Reference, actual, and estimated speed.

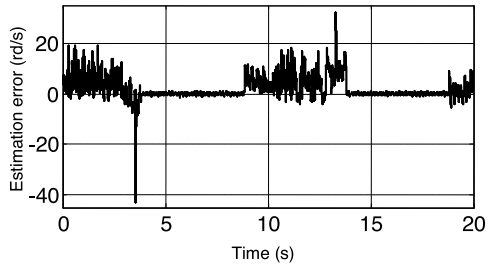

Fig. 20. Classical MRAS: Speed estimation error.

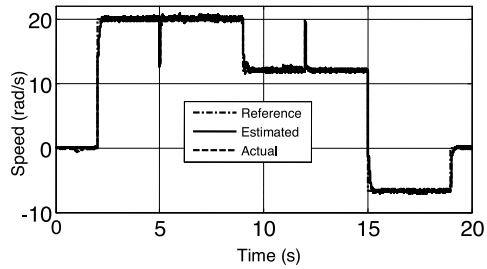

Fig. 21. Reference, actual, and estimated speed.

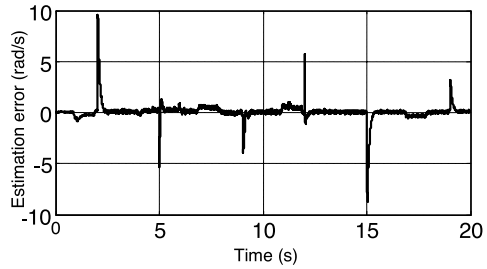

Fig. 22. Speed estimation error.

to experimentally test the robustness of our proposed control scheme, a torque load variations of 10 Nm is applied between 5 and 7 s. We can see the effect of variation load on the I_{sq} current in Fig. 17. The results show that no significant changes have affected either the speed or direct current I_{sd} of the machine [see Fig. 17]. All these tests show the robustness of the proposed observer controller scheme. Also, in Fig. 18, we can see that the *d*- and *q*-axis fluxes are decoupled and the *q*-axis flux is maintained at zero value.

To show the advantage of the proposed observer compared to the classic one, the systems responses in the first and second cases were performed. Figs. 15 and 20 show clearly that the estimated error is smallest for our proposed observer than this obtained for the classical one (Fig. 19).

To confirm the efficiency of our proposed observer at low speed regions, different speed trajectories are applied. Fig. 21 shows the reference, measured, and estimated. It is clear from this figure that the estimated and measured speeds converge to the speed reference at the same time. In Fig. 22, we can see that the estimation error is small, which proves the efficiency of the proposed MRAS even at low and zero speed regions. All these experimental results confirm the simulation results. (In this case, 10-Nm load charge was applied between 5 and 12 s).

Our control strategy has been successfully tested on dSPACE1104, which contains the Texas Instrument TMS320F240 DSP. This constructor has developed a number of DSP for industrial applications. Then, it will be easy to apply our control strategy in industry by generating C code or rewrite our algorithm in assembly language.

VI. Conclusion

In this paper, a new MRAS rotor speed observer was proposed to improve the performance of sensorless vector controller of induction machine. The control robustness is achieved by a sliding-mode controller and its stability is proved using a Lyapunov approach. Simulation and experimental results for different speed profiles had shown, on the one hand, that the proposed new MRAS observer was able to estimate accurately the actual speed at low and zero speed when the conventional MRAS observer is limited. On the other hand, the robustness of the proposed observer regarding load torque and stator resistance variations, especially at low and zero speed, is much better than the classical observer.

APPENDIX

Machine Parameters

$Rs = 5.72\,\Omega$, $Rr = 4.2\,\Omega$, $Ls = 462$ mH, $Lr = 462$ mH, $M = 440.2$ mH, $J = 0.0049$ kg·m^2, $f = 0.003$ mN·s/rd.

Rate values

$P = 1.5$ kW; $\Omega = 1430$ r/min; $I = 3.5$ A; $cos\varphi = 0.82$; pole pairs number $p = 2$; 50 Hz; load torque $= 10$ Nm.

REFERENCES

[1] J. W. Finch and D. Giaouris, "Controlled AC electrical drives," *IEEE Trans. Ind. Electron.*, vol. 55, no. 2, pp. 481–491, Feb. 2008.

[2] J.-I. Ha and S.-K. Sul, "Sensorless field-orientation control of an induction machine by high-frequency signal injection," *IEEE Trans. Ind. Appl.*, vol. 35, no. 1, pp. 45–51, Jan./Feb. 1999.

[3] C. Caruana, G.M. Asher, and M. Sumner, "Performance of high frequency signal injection techniques for zero-low-frequency vector control induction machines under sensorless conditions," *IEEE Trans. Ind. Electron.*, vol. 53, no. 1, pp. 225–238, Feb. 2006.

[4] F. Peng and T. Fukao, "Robust speed identification for speed-sensorless vector control of induction motors," *IEEE Trans. Ind. Appl.*, vol. 30, no. 5, pp. 1234–1240, Sep./Oct. 1994.

[5] C. Schauder, "Adaptive speed identification for vector control of induction motors without rotational transducers," *IEEE Trans. Ind. Appl.*, vol. 28, no. 5, pp. 1054–1061, Sep./Oct. 1992.

[6] P. Vas, *Sensorless Vector and Direct Torque Control*. New York, NY, USA: Oxford Univ. Press, 1998.

[7] S. Maiti, C. Chakraborty, Y. Hori, and M. C. Ta, "Model reference adaptive controller-based rotor resistance and speed estimation techniques for vector controlled induction motor drive utilizing reactive power," *IEEE Trans. Ind. Electron.*, vol. 55, no. 2, pp. 594–601, Feb. 2008.

[8] M. Comanescu and L. Xu, "Sliding mode MRAS speed estimators for sensorless vector control of induction machine," *IEEE Trans. Ind. Electron.*, vol. 53, no. 1, pp. 146–153, Feb. 2006.

[9] A. V. Ravi Teja, C. Chakraborty, S. Maiti, and Y. Hori, "A new model reference adaptive controller for four quadrant vector controlled induction motor drives," *IEEE Trans. Ind. Electron.*, vol. 59, no. 101, pp. 3757–3767, Apr. 2012.

[10] V. Verma, C. Chakraborty, S. Maiti, and Y. Hori, "Speed sensorless vector controlled induction motor drive using single current sensor," *IEEE Trans. Energy Convers.*, vol. 28, no. 4, pp. 938–950, Nov. 2013.

[11] C. Schauder, "Adaptive speed identification for vector control of induction motors without rotational transducers," in *Proc. IEEE Conf. Rec. Ind. Appl. Soc. Annu., Meeting*, 1989, pp. 493–499.

[12] J. Holtz and J. Quan, "Drift and parameter compensated flux estimator for persistent zero stator frequency operation of sensorless controlled induction motors," *IEEE Trans. Ind. Appl.*, vol. 39, no. 4, pp. 1052–1060, Jul./Aug. 2003.

[13] Y. A. Kwon and D. W. Jin, "A novel MRAS based speed sensorless control of induction motor," in *Proc. IEEE 25th Annu. Conf. Ind. Electron. Soc.*, 1999, pp. 933–938.

[14] Q. Gao, C. S. Staines, G. M. Asher, and M. Sumner, "Sensorless speed operation of cage induction motor using zero drift feedback integration with MRAS observer," in *Proc. Eur. Conf. Power Electron. Appl.*, 2005, pp. 1–9.

[15] M. S. Zaky, M. M. Khater, S. S. Shokralla, and H. A. Yasin, "Wide speed-range estimation with online parameter identification schemes of sensorless induction motor drives," *IEEE Trans. Ind. Electron.*, vol. 56, no. 5, pp. 1699–1707, May 2009.

[16] V. Vasic and S. Vukosavic, "Robust MRAS-based algorithm for stator resistance and rotor speed identification," *IEEE Power Eng. Rev.*, vol. 21, no. 11, pp. 39–41, Nov. 2001.

[17] L. Ben-Brahim, S. Tadakuma, and A. Akdag, "Speed control of induction motor without rotational transducers," *IEEE Trans. Ind. Appl.*, vol. 35, no. 4, pp. 844–850, Jul./Aug. 1999.

[18] M. Hinkkanen and J. Luomi, "Modified integrator for voltage model flux estimation of induction motors," *IEEE Trans. Ind. Electron.*, vol. 50, no. 4, pp. 818–820, Aug. 2003.

[19] B. Karanayil, M. F. Rahman, and C. Grantham, "An implementation of a programmable cascaded low-pass filter for a rotor flux synthesizer for an induction motor drive," *IEEE Trans. Power Electron.*, vol. 19, no. 2, pp. 257–263, Mar. 2004.

[20] S. Huang, Y. Wang, J. Gao, J. Lu, and S. Qiu "The vector control based on MRAS speed sensorless induction motor drive," in *Proc. World Congr. Intell. Control Automat.*, 2004, vol. 5, pp. 4550–4553.

[21] M. Montanari, S. Peresada, A. Tilli, A. Tonielli, "Speed sensorless control of induction motor based on indirect field-orientation," in *Proc. Ind. Appl. Conf.*, 2000, vol. 3, pp. 1858–1865.

[22] H. Khalil, *Nonlinear Systems*, 2nd ed. Englewood Cliffs, NJ, USA: Prentice-Hall, 1996.

[23] S. Drid, M. Tadjine, and M.S. Nait-Said, "Robust backstepping vector control for the doubly fed induction motor," *IET Control Theory Appl.*, vol. 1, no. 4, pp. 861–868, 2007.

[24] D. Khamari, A. Makouf, S. Drid, and L. Chrifi-Alaoui, "High performance of self-scheduled linear parameter varying control with flux observer of induction motor," *J. Elect. Eng. Technol.*, vol. 8, no. 5, pp. 1202–1211, 2013.

[25] Z. Li, Z. Liu, L. Diao, W. Lin, and G. Zhang, "A sensorless vector control of induction machines based on hybrid model," in *Proc. Int. Conf. Ind. Electron. Appl.*, 2007, pp. 1188–1192.

[26] J. Holtz, "Sensorless position control of induction motors—An emerging technology" in *Proc. Int. Conf. Ind. Electron., Control, Instrum.*, Aachen, Germany, Aug. 31–Sep. 4, 1993, pp. 11–112.

[27] C. Ilas, A. Bettini, L. Ferraris, G. Griva, and F. Profumo, "Comparision of different schemes without shaft sensors for field oriented control drives," in *Proc. Int. Conf. Ind. Electron., Control, Instrum.*, 1994, pp. 1579–1588.

Idriss Benlaloui was born in Batna, Algeria, in 1988. He received the B.Sc. and M.Sc. degrees in electrical engineering from the University of Batna, Batna, in 2009 and 2011, respectively. He is currently working toward the Ph.D. degree at the Electrical Engineering Institute, University of Batna.

Mr. Benlaloui is a Member of the Research Laboratory of Electromagnetic Induction and Propulsion Systems, University of Batna.

Saïd Drid (SM'13) was born in Batna, Algeria, in 1969. He received the B.Sc., M.Sc., and Ph.D. degrees in electrical engineering from the University of Batna, Batna, in 1994, 2000, and 2005, respectively.

He is currently a full Professor at the Electrical Engineering Institute, University of Batna. He is the Head of the Energy Saving and Renewable Energy Team, Research Laboratory of Electromagnetic Induction and Propulsion Systems, University of Batna. His research interests include electric machines and drives, and renewable energy. He is also a reviewer for some international journals.

Dr. Drid is a Member of the IEEE Power and Energy Society (PES). He is currently the Vice Chair of the PES chapter, IEEE Algeria section.

Larbi Chrifi-Alaoui received the Ph.D. degree in automatic control from the Ecole Centrale de Lyon, Écully, France, in 1994.

Since 1999, he has held a teaching position in automatic control at the Aisne University Institute of Technology, Université de Picardie Jules Verne, Cuffies-Soissons, France, where, from 2004 to 2010, he was the Head of the Department of Electrical Engineering and Industrial Informatics. His research interests include linear and nonlinear control theory, including sliding mode control, adaptive control, and robust control, with applications to electric drive and mechatronics systems.

Mohammed Ouriagli received the Ph.D. degree in electrical engineering from the Institut National Polytechnique de Lorraine, Lorraine, France, in 1995.

Since 2003, he has held a teaching position in automatic control in the Polydisciplinary Faculty of Taza, Université Sidi Mohamed Ben-Abdellah (USMBA), Taza, Morroco. His research interests mainly include linear and nonlinear control theory, including sliding mode control, adaptive control, robust control, electric drive applications, and mechatronics systems.